

# Modeling of single pole write head and double-layered medium for 3-D eddy current analysis

Yasushi Kanai<sup>a,\*</sup>, Ryo Matsubara<sup>a</sup>, Hiroaki Muraoka<sup>b</sup> and Yoshihisa Nakamura<sup>b</sup>

<sup>a</sup>*Department of Information and Electronics Engineering, Faculty of Engineering, Niigata Institute of Technology, 1719 Fujihashi, Kashiwazaki 945-1195, Japan*

<sup>b</sup>*Research Institute of Electrical Communication, Tohoku University, Katahira 2-1-1, Aoba-ku, Sendai 980-8577, Japan*

**Abstract.** Finite-element modeling of single pole (SPT) write head with double-layered medium for perpendicular magnetic recording is investigated. In carrying out 3-D eddy current transient finite-element analysis, reducing the medium area is one key factor for computation time reduction while maintaining sufficient solution accuracy. It is also investigated the number of layer divisions for thin metallic under-layer. The results validate the modeling of SPT head with double-layered medium.

Keywords: Perpendicular magnetic recording, write heads, high frequency recording, finite element methods, model validation

## 1. Introduction

Perpendicular magnetic recording of 98.9 Mb/mm<sup>2</sup> (63.8 Gb/in<sup>2</sup>) was demonstrated using a single-pole (SPT) head with a double-layered medium [1]. Consequent key areas of interest are high frequency response and recording field strength in a narrow track width to achieve areal densities greater than 155 Mb/mm<sup>2</sup> (100 Gb/in<sup>2</sup>). Finite element method is one of the best tools to analyze head fields [2]. However, modeling the SPT head along with a double-layered medium for 3-D eddy current analysis has not been fully reported.

In this paper, finite element model validity for the SPT head with a double-layered medium is investigated. In perpendicular recordings, unlike the longitudinal one, double-layered (recording- and soft under-layers) medium is usually used. Modeling the soft magnetic under-layer is necessary because interaction between the SPT head and soft magnetic under-layer is strong. However, the ratio of 3.5-inch disk-shaped medium and recording-layer thickness of 20 nm is extremely large, therefore, it is impossible to model the whole medium. In other words, reducing medium area is one of the key factors for computation time reduction while maintaining sufficient solution accuracy. To consider the eddy current effect accurately, it is necessary to divide the metallic under-layer into very thin layers. However, it has not been clear how thin the division of under-layer should be compared to the skin depth practically. Therefore, the solution accuracy is investigated by varying the number of layer divisions, conductivity and frequency. The results give a criterion for eddy current analysis of SPT head with double-layered medium.

---

\*Corresponding author: Yasushi Kanai, Tel.: +81 257 22 8127; Fax: +81 257 22 8122; E-mail: kanai@iee.niit.ac.jp.

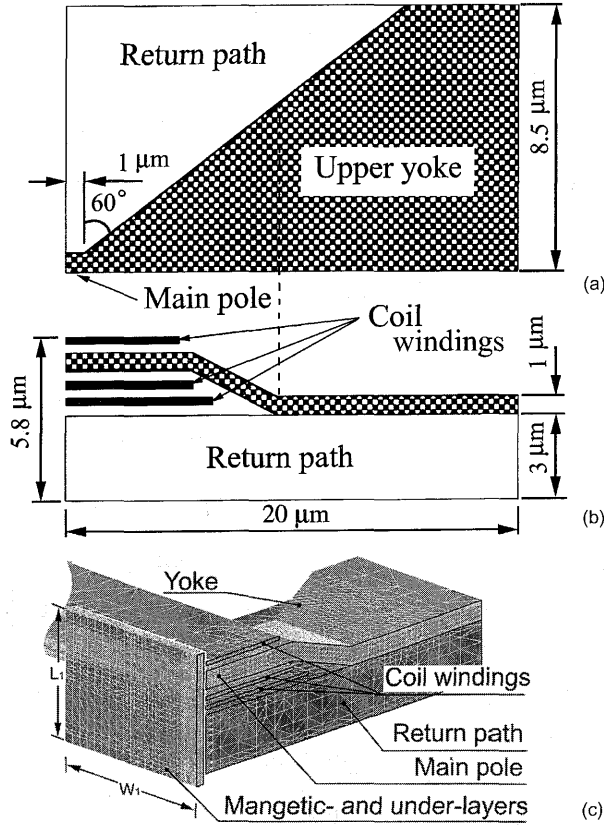


Fig. 1. SPT head model used for calculations. a) plan view, b) side view, c) finite-element mesh of SPT head with a double-layered medium.

## 2. Finite-element modeling accuracy: medium area

JMAG-Works [3], FEM commercial software, is used to analyze the head field throughout this paper. The equations solved are

$$\nabla_{\mathbf{x}} \left( \frac{1}{\mu} \nabla_{\mathbf{x}} \mathbf{A} \right) = \mathbf{J}_0 - \sigma \left( \frac{\partial \mathbf{A}}{\partial t} + \nabla \phi \right) \quad (1)$$

$$\nabla \cdot \left\{ \left( -\sigma \left( \frac{\partial \mathbf{A}}{\partial t} + \nabla \phi \right) \right) \right\} = 0 \quad (2)$$

where,  $\mu$ ,  $\mathbf{A}$ ,  $\sigma$  and  $\phi$  are permeability, magnetic vector potential, current density, conductivity and electrical scalar potential. Convergence criteria for ICCG and Newton-Raphson nonlinear iterations are set to be  $10^{-7}$  and  $10^{-3}$ , respectively to obtain the accurate solution [4]. Material nonlinearity and eddy currents are considered in calculations while magnetic resonance, magnetic anisotropy, hysteresis and displacement current are ignored.

Figures 1(a)–(c) show the schematic structure of the SPT head and a finite element model with a double-layered medium. Table 1 shows major parameters used for calculations with specifications given for higher densities than previously reported [5]: soft material with 1.8 T saturation magnetization

Table 1  
Major specifications used for calculations

Main pole	Thickness	1.0 $\mu\text{m}$
	Track width	0.1 $\mu\text{m}$
	Mp length	1 $\mu\text{m}$
	Saturation	1.8 T
	Conductivity	$1.5 \times 10^6$ S/m
	Initial relative permeability	1000
	Magnetic space	15 nm
Medium	Thickness	20 nm
	Initial relative permeability	2
Under-layer	Thickness	600 nm
	Saturation	1.8 T
	Conductivity	$1.5 \times 10^6$ S/m
	Initial relative permeability	1000

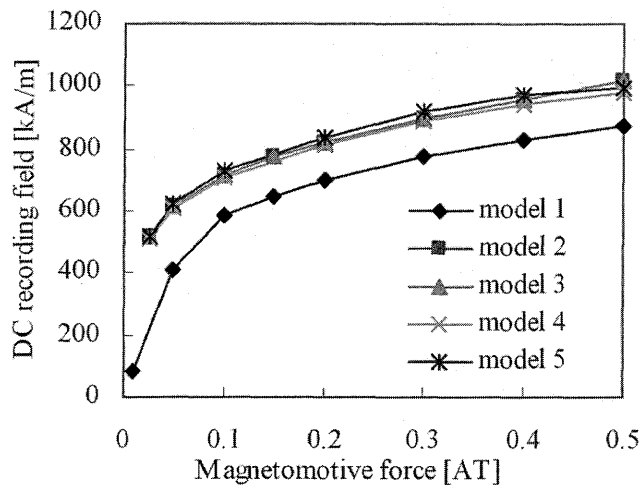


Fig. 2. DC recording field vs. MMF for various models.

and  $1.5 \times 10^6$  S/m conductivity is under development. Modeling the soft magnetic under-layer is essential due to strong interaction between the SPT head and the soft magnetic under-layer. Note that the intermediate layer, usually deposited between the under- and recording-layers, is ignored for modeling.

Taking advantage of geometrical symmetry, the half region is discretized. Calculation time is strongly dependent upon medium area; therefore, it is essential to optimize medium area. In other words, one needs to reduce calculation time by minimizing the medium area with maintaining sufficient accuracy of the solution. Table 2 shows five models used for calculation. The area of  $6.8 \mu\text{m} \times 9.0 \mu\text{m}$  ( $W_1 \times L_1$  and  $W_2 \times L_2$  in Fig. 1(c)) covers the main pole and return path exposed to air bearing surface (ABS). Note that wider medium area, such as  $25 \mu\text{m} \times 50 \mu\text{m}$  ( $W_1 \times L_1$  and  $W_2 \times L_2$  in Fig. 1(c)), gives no solution change. The under-layer is divided into four layers, which will be discussed in the next section. The DC recording field vs. magnetomotive force (MMF) is shown in Fig. 2. From this figure, it is evident that models 3–5 have sufficient accuracy while models 1 and 2 are inadequate. Figure 3 shows the DC head field distributions in the recording-layer when medium area is  $25 \mu\text{m} \times 25 \mu\text{m}$ , showing the flux density becomes small sharply outside the main pole and return path region. Therefore, medium area of  $6.8 \mu\text{m} \times 9.0 \mu\text{m}$  is enough with regard to the accuracy of recording head field.

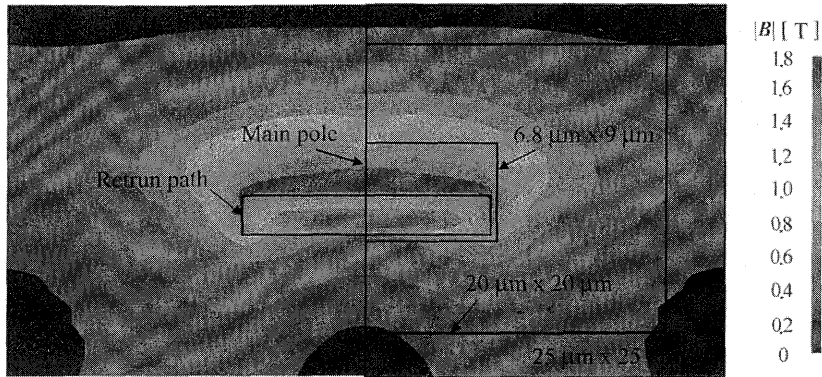


Fig. 3. DC recording field distribution  $|B|$  in the under-layer for model 3 along with head structure exposed to air bearing surface (ABS).

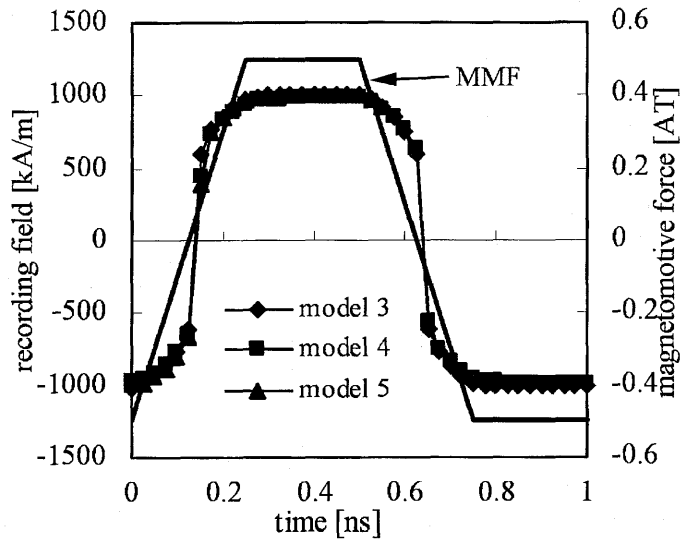


Fig. 4. Head field time dependence for models 3–5.

Calculation times for models 1–5 when MMF of 0.5 AT is applied are 18 min, 1.0, 3.4, 4.6 and 25 hrs on a Pentium III (933 MHz): model 5 should be removed from consideration due to long calculation time. Note that the reason of long calculation time is the increase of ICCG iterations as the increase of medium area. The calculation times of 5- to 10-fold are required when compared to those of the longitudinal recording write heads with the same number of tetrahedral elements.

Figure 4 shows the head field time dependence for models 3–5 with 1 GHz MMF driving. Transient analyses are carried out through division of one cycle into 41 steps. Note that we have carried out the analyses through division 81, and confirmed that 41 steps are enough to obtain the accurate solutions. From the same figure, major head field differences between models 3–5 are not found; therefore, a sufficiently accurate solution can be obtained using models 3–5. In Fig. 5, head field distributions are shown in the recording-layer for 1 GHz at  $t = 0.25$  ns (see Fig. 4) when medium areas are  $25 \mu\text{m} \times 25 \mu\text{m}$  (upper) and  $20 \mu\text{m} \times 20 \mu\text{m}$ , showing no major difference between these two figures around the main pole. As in the DC case, the medium area of  $6.8 \mu\text{m} \times 9.0 \mu\text{m}$  is enough with regard to the accuracy of

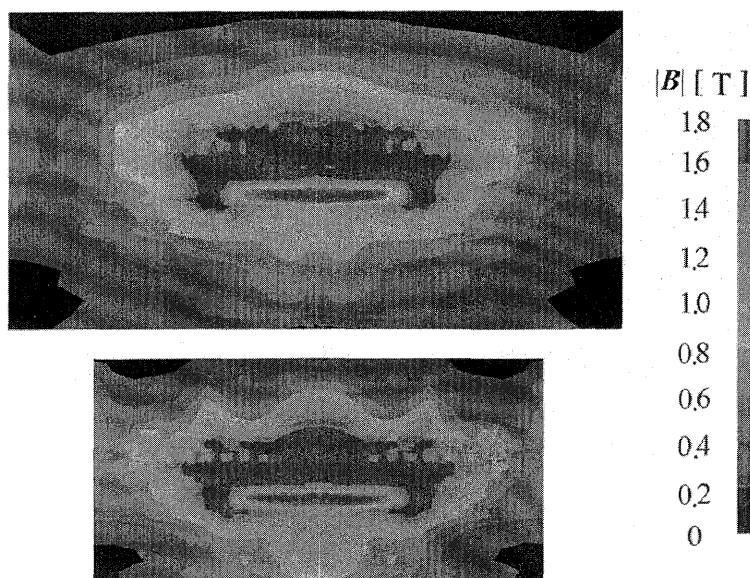


Fig. 5. Magnetic flux distribution  $|B|$  in the under-layer for model 3.1 GHz,  $t = 0.25$  ns in Fig. 4. Medium area considered; upper:  $25 \mu\text{m} \times 25 \mu\text{m}$ , lower:  $20 \mu\text{m} \times 20 \mu\text{m}$ .

recording head field. In Fig. 6, eddy current distributions in the under-layer surface are shown for 1 GHz at  $t = 0.25$  ns (see Fig. 4) when medium areas are  $25 \mu\text{m} \times 25 \mu\text{m}$  (upper) and  $20 \mu\text{m} \times 20 \mu\text{m}$ , showing no major difference between these two figures around the main pole. These figures show that the eddy current flows around the main pole and return path, therefore, the medium area of  $6.8 \mu\text{m} \times 9.0 \mu\text{m}$  that covers the main pole and return path exposed to the air bearing surface (ABS) is enough. Calculation times for models 3–5 are 67, 118 and 495 hrs on the same PC. Note that the reason of long calculation time is the increase of ICCG and nonlinear iterations. As noted earlier, models 1 and 2 were ignored as inadequate. From study in this section, optimum medium area to reduce computation time while maintaining sufficient solution accuracy is obtained with  $6.8 \mu\text{m} \times 9.0 \mu\text{m}$ : therefore, model 3 with  $6.8 \mu\text{m} \times 9.0 \mu\text{m}$  medium area is used hereafter.

### 3. Finite-element modeling accuracy: division number of layers for metallic under-layer

The delay of recording field due to eddy current that flows in the metallic under-layer has been considered as a big issue. As can be seen from Fig. 4, the concerns have been eliminated because the recording field well follows the driving. However, the question arises whether the calculations with division of the soft magnetic under-layer into four layers are accurate.

Here, we investigate the solution accuracy by varying the number of layer divisions, conductivity and frequency. Then, we divide the under-layer into ten layers so that we can consider the eddy current phenomenon properly. In this model, the number of tetrahedral elements was 1,051,529. Therefore, more than 600,000 additional tetrahedral elements were used to model the under-layer. In Figs 7 and 8, the head field time dependences are shown for the four- and ten-layered under-layers with conductivity  $\sigma$  of  $5 \times 10^6$  and  $1.5 \times 10^6$  S/m. It should be noted that the horizontal axes are normalized to understand the delay of recording field. No major difference distinguished results were obtained for conductivity  $\sigma$  of  $1.5 \times 10^6$  S/m. On the other hand, the calculation is not accurate for  $5 \times 10^6$  S/m at 1 GHz and

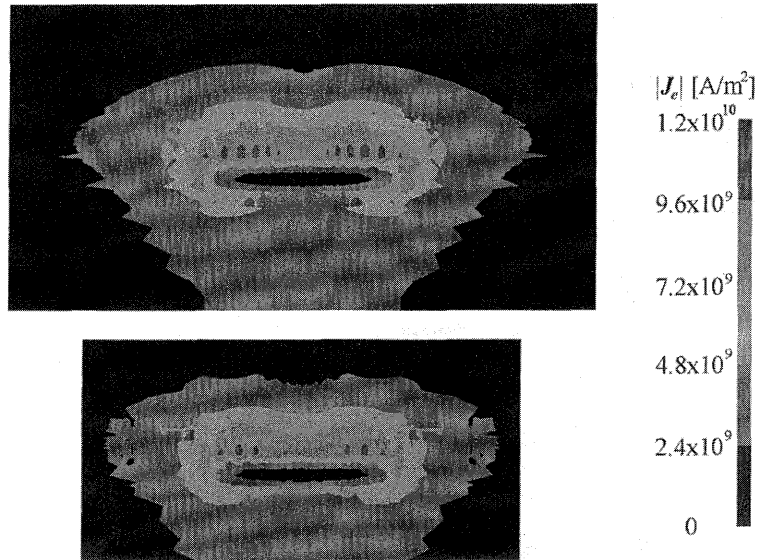


Fig. 6. Eddy current distribution  $|J_e|$  in the under-layer for model 3.1 GHz,  $t = 0.25$  ns in Fig. 4. Medium area considered; upper:  $25 \mu\text{m} \times 25 \mu\text{m}$ , lower:  $20 \mu\text{m} \times 20 \mu\text{m}$ .

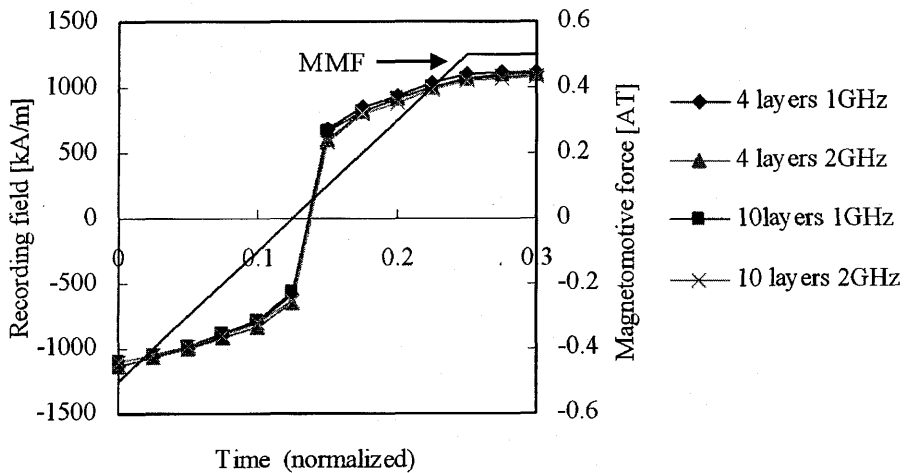


Fig. 7. Head field time dependence for first 13 steps in 41 full steps. Conductivity of under-layer:  $1.5 \times 10^6$  S/m. Number of layers of under-layer: 4 and 10. Frequency: 1 and 2 GHz. Horizontal axis (time) is normalized.

it is not acceptable when recording frequency of 2 GHz is applied. Note that the skin depth is 159 nm for frequency of 2 GHz, conductivity of  $5 \times 10^6$  S/m and relative permeability of 1000. From these calculations, the accuracy of eddy current analysis can be estimated for later studies [6].

The calculation times and memory requirements are shown in Table 3. Note that maximum ICCG iterations are 186 for four-layered division and 455 and ten-layered division, respectively; nonlinear iterations are 5–9 time for four-layered division and 8–17 times for ten-layered division. This means that thin elements in under-layer leads to deterioration of the ICCG and nonlinear convergence.

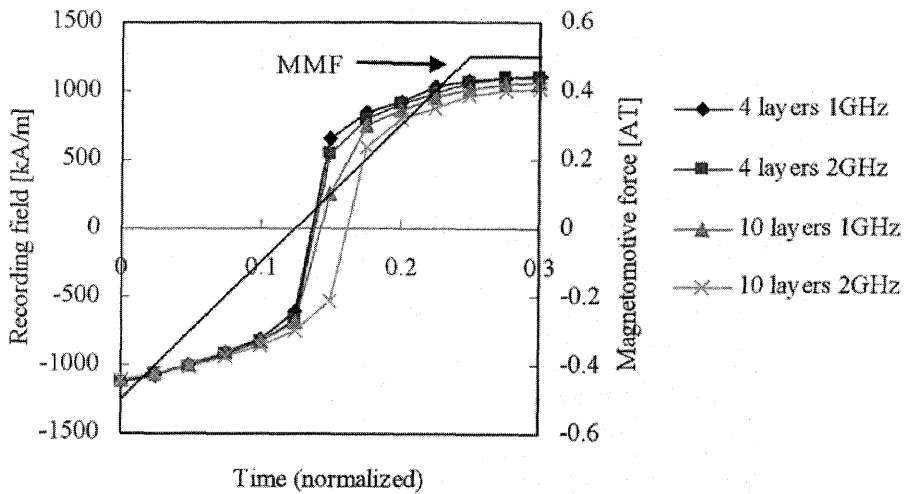


Fig. 8. Head field time dependence for first 13 steps in 41 full-steps. Conductivity of under-layer:  $5 \times 10^6$  S/m. Number of layers of under-layer: 4 and 10. Frequency: 1 and 2 GHz. Horizontal axis (time) is normalized.

Table 2  
Area of under- and recording- layers ( $L_1 \times W_1$  and  $L_2 \times W_2$ ) for models 1–5

Model id #	$L_1 \times W_1$	$L_2 \times W_2$	No. of element
1	$1.5 \mu\text{m} \times 2 \mu\text{m}$	$1.5 \mu\text{m} \times 2 \mu\text{m}$	246,790
2	$6.8 \mu\text{m} \times 9 \mu\text{m}$	*note	294,790
3	$6.8 \mu\text{m} \times 9 \mu\text{m}$	$6.8 \mu\text{m} \times 9 \mu\text{m}$	326,500
4	$20 \mu\text{m} \times 20 \mu\text{m}$	$20 \mu\text{m} \times 20 \mu\text{m}$	395,661
5	$25 \mu\text{m} \times 25 \mu\text{m}$	$25 \mu\text{m} \times 25 \mu\text{m}$	465,414

\*note: recording track ( $6.8 \mu\text{m} \times 0.05 \mu\text{m}$ ) and main pole neighbor ( $1.0 \mu\text{m} \times 1.2 \mu\text{m}$ ) is modeled.

Table 3  
Calculation time and memory required. Frequency: 2 GHz, medium area:  $6.8 \mu\text{m} \times 9.0 \mu\text{m}$ , under-layer conductivity:  $1.5 \times 10^6$  S/m

	No of elements	Memory[MB]	CPU time [hrs]
4 Layers	330,405	186	38
10 Layers	1,051,529	642	304

#### 4. Conclusion

Finite element model validity for the single-pole (SPT) write head with a double-layered medium is investigated. In calculating SPT head with double-layered medium, special care has to be taken to the medium area. Calculation time was reduced by finite-element model validation. The accuracy of eddy current analysis has been investigated by varying the layer numbers of under-layer, recording frequency, conductivity of under-layer. The results give a criterion for eddy current analysis of SPT with double-layered medium.

## Acknowledgment

This work was supported in part by a Grant in Aid for Scientific Research of the Japan Society for the Promotion of Science (#12,650,351) and Storage Research Consortium (SRC), Japan. The authors also wish to acknowledge use of JMAG-Works from The Japan Research Institute, Limited.

## References

- [1] H. Takano, Y. Nishida, A. Kuroda, H. Sawaguchi, T. Kawabe, A. Ishikawa, H. Aoi, H. Muraoka, Y. Nakamura and K. Ouchi, The 8th Joint MMM-Intermag Conf, 2001, CA-01.
- [2] Y. Kanai, R. Matsubara, H. Muraoka and Y. Nakamura, The 8th Joint MMM-Intermag Conf, 2001, FR-13.
- [3] JMAG-works, commercial software, The Japan Research Institute, Ltd. (<http://www.jri.co.jp/pro-eng/jmag/E/index.html>)
- [4] K. Fujiwara, F. Ikeda, A. Kameari, Y. Kanai, K. Nakamura, N. Takahashi, K. Tani and T. Yamada, *IEEE Trans. Magn* **36** (2000) 1784.
- [5] H. Muraoka, K. Sato, Y. Nakamura, T. Katakura and K. Yoshizawa, *IEEE Trans. Magn* **34** (1998) 1474.
- [6] Y. Kanai and R. Matsubara, The Magnetic Recording Conference, 2001, F-4.